COMPARING MULTIVARIATE COMPLEX RANDOM SIGNALS: PERFORMANCE ANALYSIS AND APPLICATION

Jitendra K. Tugnait

Department of Electrical and Computer Engineering
Auburn University, Auburn, AL 36849, USA
tugnajk@eng.auburn.edu

ABSTRACT

We consider a recently proposed generalized likelihood ratio test (GLRT) for comparing two complex multivariate random signal realizations to ascertain whether they have identical power spectral densities. In this paper we analyze the performance of this GLRT by deriving an approximate asymptotic distribution of the test statistic under the alternative hypothesis. We also provide robustification of this approach by adding artificial white noise to the received noisy signals. The results are illustrated via computer simulations which include application to user authentication in wireless networks with multiantenna receivers.

***Index Terms*—** Multichannel signal detection; GLRT; wireless user authentication; multiple antennas.

1. INTRODUCTION

This paper is concerned with comparison of two realizations (sample functions) of some random signals (time series) to assess if they are realizations of the same random signal. The main motivation for this paper is potential application to two areas: (i) user authentication for wireless network security enhancement at the physical layer, and (ii) spectrum sensing (looking for presence/absence of primary users (PUs) in spectral bands) in cognitive radio (CR) networks (based on the two-window approach of [11]).

Relation to Prior Work Recent general articles on comparison of random signals include [4], [7], [10], and references therein. These approaches are focused on stationary signals exploiting their second-order properties (power spectral densities (PSD) or correlation functions). Our focus will also be on such a class of signals. Also, these approaches are limited to either real-valued scalar time series [4], [7] or to real-valued multivariate processes [10]. In [12] we have investigated scalar complex-valued random signals and extended the theory of [12] to multivariate complex-valued random signals in [13]. In [13] a GLRT is presented and an analytical method for threshold calculation is offered. However, [13] does not provide any performance analysis. A goal of this paper is to analyze the detection performance of the GLRT proposed in [13]. We also provide robustification of this approach by adding artificial white noise to the received signals. The results are illustrated via simulations which include application to user authentication in wireless networks with multiantenna receivers (extending the single antenna results of [14]).

Notation: $|\mathbf{A}|$ and $\mathrm{etr}(\mathbf{A})$ denote the determinant and the exponential of the trace of the square matrix $\mathbf{A}$, respectively; i.e. $\mathrm{etr}(\mathbf{A}) = \exp(\mathrm{tr}(\mathbf{A}))$. $\mathbf{B}_{ij}$ denotes the ijth element of the matrix $\mathbf{B}$ and $\mathbf{I}$ is the identity matrix. The superscripts $*$ and H denote the complex conjugate and the Hermitian (conjugate transpose) operations, respectively. The notation $y = \mathcal{O}(g(x))$ means that there exists some finite real number $b > 0$ such that $\lim_{x\to\infty} |y/g(x)| \le b$. Given a column vector $\mathbf{x}$, diag$\{\mathbf{x}\}$ denotes a square matrix with elements of $\mathbf{x}$ along its main diagonal and zeros everywhere else. $\delta(\tau)$ denotes the Kronecker delta, i.e. $\delta(\tau) = 1$ if $\tau = 0, = 0$ otherwise. Given two random vectors $\mathbf{x}$ and $\mathbf{y}$, we define $\mathrm{cov}(\mathbf{x}, \mathbf{y}) := E\{\mathbf{x}\mathbf{y}^H\} - E\{\mathbf{x}\}E\{\mathbf{y}^H\}$. We use χ^2_n to denote a random variable with central chi-square distribution with n degrees of freedom (as well as the distribution itself).

2. SYSTEM MODEL

We consider two zero-mean (proper) complex multivariate (dimension p) stationary random signals $\{\mathbf{x}(t)\}$ and $\{\mathbf{y}(t)\}$ with $p \times p$ PSD matrices $\mathbf{S}_x(f)$ and $\mathbf{S}_y(f)$, respectively. We observe the two processes for $t = 0, 1, \cdots, N-1$ (N samples each). We employ multivariate spectral analysis to test if the two sets of observation are realizations of two random signals with identical PSDs. We will assume that both $\mathbf{x}(t)$ and $\mathbf{y}(t)$ are stationary with all bounded moments so that some asymptotic results from [2] regarding PSD estimators can be invoked; the time series need not be Gaussian. Numerous approaches are available ([2, 9]) to estimate $\mathbf{S}(f)$ on a grid $f_n := n/N$, $n = 0, 1, \cdots, N-1$. A key fact is that at any frequency f (on the appropriate FFT grid in the interval $[0, 2\pi) \equiv [0, 1.0)$), e.g. for $f_k = k/N$, $k \in [1, N-1]$, the PSD estimator $\hat{\mathbf{S}}(f)$ of the true $p \times p$ PSD matrix $\mathbf{S}(f)$ has the (asymptotic: N "large") distribution

$$\hat{\mathbf{S}}(f) \sim (1/K) W_C \left(p, K, \mathbf{S}(f)\right) \tag{1}$$

where, in the Welch method, K ($\ge p$) is the number of data segments and in the Daniell method it is the number of frequency bins over which the periodogram is averaged, and

$W_C(p, K, \mathbf{S}(f))$ denotes the complex Wishart distribution of dimension p and degrees of freedom K. We will use the Daniell method for PSD estimation. In this method, given $p \times 1$ time series $\mathbf{x}(t)$, $t = 0, 1, \cdots, N-1$, we first compute the periodogram as $\hat{\mathbf{S}}_p(f_n) = N^{-1}\mathbf{I}(f)\mathbf{I}^H(f)$, $\mathbf{I}(f) := \sum_{t=0}^{N-1} \mathbf{x}(t)e^{-j2\pi f_n t}$. Then the PSD estimator is computed as $\hat{\mathbf{S}}(f_n) = \frac{1}{K}\sum_{l=-m_t}^{m_t} \hat{\mathbf{S}}_p(f_{n+l})$ where $K = 2m_t + 1$.

If $\mathbf{X} \sim W_C(p, K, \mathbf{S}(f))$, then $\mathbf{A}\mathbf{X}\mathbf{A}^H \sim W_C(m, K, \mathbf{A}\mathbf{S}(f)\mathbf{A}^H)$ for any $m \times p$ matrix $\mathbf{A}$ of rank m.. We will denote the spectral estimator at the k-th frequency bin (f_k) acquired from $\{\mathbf{x}(t)\}$, $(t = 0, 1, \cdots, N-1)$, as $\mathbf{X}_k$ and that acquired from $\{\mathbf{y}(t)\}$ as $\mathbf{Y}_k$, with their true values denoted as $\mathbf{S}_x(f_k)$ and $\mathbf{S}_y(f_k)$, respectively. Thus,

$$\mathbf{X}_k \sim \frac{1}{K}W_C(p, K, \mathbf{S}_x(f_k)), \; \mathbf{Y}_k \sim \frac{1}{K}W_C(p, K, \mathbf{S}_y(f_k)) \tag{2}$$

and the two are assumed to be independent. We confine attention to frequency points over which the spectral estimators are mutually independent, which for the Daniell method are given by $f_k = (kK + \lceil(K/2)\rceil)/N$, $k \in [0, \lfloor(N-(K/2)-1)/K\rfloor]$. Let $\mathcal{M} := \{f_k : k_0 \le k \le k_0 + M - 1\}$ denote the set of M frequency bins that specify the frequency band of interest; without loss of generality, we will reindex the frequency subscripts to run from 1 through M.

3. P.S.D.-BASED G.L.R.T.

The binary hypothesis testing problem in this case is

$$\begin{array}{ll} \mathcal{H}_0: & \mathbf{S}_y(f_k) = \mathbf{S}_x(f_k) = \mathbf{S}(f_k) \; \forall f_k \in \mathcal{M} \\ \mathcal{H}_1: & \mathcal{H}_0^c = \text{complement of } \mathcal{H}_0 \end{array} \tag{3}$$

given the "data" $\mathbf{X}_k$ and $\mathbf{Y}_k$, where the unknown parameters are $\mathbf{S}_x(f_k)$ and $\mathbf{S}_y(f_k)$, $f_k \in \mathcal{M}$. This problem has been considered in [13] for comparing two complex multivariate random signals and the resulting GLRT is

$$\mathcal{L}(\mathbf{X}, \mathbf{Y}) := \prod_{k=1}^{M} \frac{\left|\frac{\mathbf{X}_k + \mathbf{Y}_k}{2}\right|^{2K}}{|\mathbf{X}_k|^K \, |\mathbf{Y}_k|^K} \underset{\mathcal{H}_0}{\overset{\mathcal{H}_1}{\gtrless}} \tau, \tag{4}$$

where the threshold τ is picked to achieve a given probability of false alarm $P_{fa} = P\{\mathcal{L}(\mathbf{X}, \mathbf{Y}) \ge \tau \,|\, \mathcal{H}_0\}$. This requires pdf of $\mathcal{L}(\mathbf{X}, \mathbf{Y})$ under $\mathcal{H}_0$. To this end we can establish Theorem 1 [13]. First some notation and definitions. Let $B_r(h)$ denote the Bernoulli polynomial of degree r and order unity. Define

$$f = p^2 M, \quad \rho = 1 - \frac{2p^2 - 1}{4pK}, \tag{5}$$

$$\omega_r = \frac{(-1)^{r+1} M}{r(r+1)(\rho K)^r} \sum_{l=1}^{p} \Big\{ 2B_{r+1}((1-\rho)K + 1 - l) - \frac{1}{2^r} B_{r+1}(2(1-\rho)K + 1 - l) \Big\}, \tag{6}$$

$$\ln(\mathcal{L}) = K\Big(-2pM\ln(2) + \sum_{k=1}^{M} \big\{ 2\ln(|\mathbf{X}_k + \mathbf{Y}_k|) - \ln(|\mathbf{X}_k|) - \ln(|\mathbf{Y}_k|) \big\} \Big). \tag{7}$$

Theorem 1 [13] . The GLRT for the binary hypothesis testing problem (3) is given by $2\rho\,\ln(\mathcal{L}) \underset{\mathcal{H}_0}{\overset{\mathcal{H}_1}{\gtrless}} \tau$ where ρ and $\ln(\mathcal{L})$ are given by (5) and (7), respectively. The threshold τ is picked to achieve a pre-specified probability of false alarm $P_{fa} = P\{2\rho\,\ln(\mathcal{L}) > \tau \,|\, \mathcal{H}_0\} = 1 - P\{2\rho\,\ln(\mathcal{L}) \le \tau \,|\, \mathcal{H}_0\}$. The probability $P\{2\rho\,\ln(\mathcal{L}) \le \tau \,|\, \mathcal{H}_0\}$ is given by (8):

$$\begin{aligned} P\{2\rho\,\ln(\mathcal{L}) \le z \,|\, \mathcal{H}_0\} &= P\{\chi_f^2 \le z\} + \omega_2 \left[P\{\chi_{f+4}^2 \le z\} - P\{\chi_f^2 \le z\}\right] + \omega_3 \left[P\{\chi_{f+6}^2 \le z\} - P\{\chi_f^2 \le z\}\right] \\ &+ \Big\{ \omega_4 \left[P\{\chi_{f+8}^2 \le z\} - P\{\chi_f^2 \le z\}\right] + \frac{1}{2}\omega_2^2 \left[P\{\chi_{f+8}^2 \le z\} - 2P\{\chi_{f+4}^2 \le z\} + P\{\chi_f^2 \le z\}\right] \Big\} \\ &+ \mathcal{O}(K^{-5}) \qquad \Box \end{aligned} \tag{8}$$

Theorem 1 allows us to calculate the test threshold "analytically" instead of via simulations.

4. ROBUSTIFICATION/REGULARIZATION

When the PSD of the signals is "small" at certain frequencies (i.e. $|\mathbf{X}_k|$ and/or $|\mathbf{Y}_k|$ in (4)), the test statistic may be unduly influenced by these frequencies. One solution to alleviate this is to add artificial noise to both $\mathbf{x}(t)$ and $\mathbf{y}(t)$ to define

$$\tilde{\mathbf{x}}(t) = \mathbf{x}(t) + \mathbf{w}_x(t), \;\; \tilde{\mathbf{y}}(t) = \mathbf{y}(t) + \mathbf{w}_y(t)$$

where $\mathbf{w}_x(t)$ and $\mathbf{w}_y(t)$ are independent zero-mean complex white Gaussian artificial noise sequences with $E\{\mathbf{w}_x(t)\mathbf{w}_x^H(t+\tau)\} = \sigma_{wx}^2\mathbf{I}\delta(\tau)$, $E\{\mathbf{w}_y(t)\mathbf{w}_y^H(t+\tau)\} = \sigma_{wy}^2\mathbf{I}\delta(\tau)$. Also, for slowly time-varying processes (e.g. output of slowly time-varying communications channels), addition of stationary artificial noise makes the test more tolerant of discrepancies between the PSDs over the two realizations. In our simulations we picked $\sigma_{wx}^2 = 0.1E\{\mathbf{x}(t)\mathbf{x}^H(t)\}/p$ and $\sigma_{wy}^2 = 0.1E\{\mathbf{y}(t)\mathbf{y}^H(t)\}/p$ ("10% noise"). For test implementation and analysis we use $\tilde{\mathbf{x}}(t)$ and $\tilde{\mathbf{y}}(t)$ instead of $\mathbf{x}(t)$ and $\mathbf{y}(t)$, respectively.

5. PROBABILITY OF DETECTION

Under "local" alternatives, using [5] and [3, Chapter 22], it follows that asymptotically (as N, M, K all $\to \infty$) under $\mathcal{H}_1$, $2\,\ln(\mathcal{L}(\mathbf{X}, \mathbf{Y})) \sim \chi_{Mp^2}^2(\lambda)$, and $2\,\ln(\mathcal{L}(\mathbf{X}, \mathbf{Y})) \sim \chi_{Mp^2}^2$ under $\mathcal{H}_0$, where $\chi_n^2(\lambda)$ denotes the non-central chi-square distribution with n degrees of freedom and non-centrality parameter λ. Typically (see [5] and [3, Chapter 22], for instance) one calculates the first- and second-order derivatives of the log-likelihood ratio and then take their expectation (essentially one needs the Fisher information matrix in order to compute λ). We will follow an indirect approach to compute λ (also used in [14] for scalar signals). We note that asymptotically, under $\mathcal{H}_1$, we must have $E\{2\,\ln(\mathcal{L}(\mathbf{X}, \mathbf{Y}))\} =$

$Mp^2 + \lambda$ since $2\,\ln(\mathcal{L}(\mathbf{X},\mathbf{Y})) \sim \chi^2_{Mp^2}(\lambda)$. We now derive an expression for the non-centrality parameter λ via $E\{2\,\ln(\mathcal{L}(\mathbf{X},\mathbf{Y}))\}$.

Consider the test statistic in (7) under $\mathcal{H}_1$. Under $\mathcal{H}_1$, the distributions of $\mathbf{X}_k$ and $\mathbf{Y}_k$ are given by (2), where $\mathbf{S}_x(f_k)$ and $\mathbf{S}_y(f_k)$ are, in general, different. We also need the distribution of $\mathbf{Z}_k = (\mathbf{X}_k + \mathbf{Y}_k)/2$ under $\mathcal{H}_1$.

Lemma 1. Under $\mathcal{H}_1$, approximately

$$\mathbf{Z}_k := (\mathbf{X}_k + \mathbf{Y}_k)/2 \sim W_C\left(p, d_k K, \frac{\mathbf{S}_x(f_k)+\mathbf{S}_y(f_k)}{2d_kK}\right) \tag{9}$$

where $\bar{\mathbf{S}}_k = \mathbf{S}_x(f_k) + \mathbf{S}_y(f_k))/2$ and

$$d_k = \frac{\mathrm{tr}(\bar{\mathbf{S}}_k^2) + \left(\mathrm{tr}(\bar{\mathbf{S}}_k)\right)^2}{\mathrm{tr}(\mathbf{S}_x^2(f_k)+\mathbf{S}_y^2(f_k)) + (\mathrm{tr}(\mathbf{S}_x(f_k)))^2 + (\mathrm{tr}(\mathbf{S}_y(f_k)))^2} \tag{10}$$

Proof. See [8, Sec. 3]. $\square$

By (9) and [1, Theorem 3.8, p. 51], we have

$$|\mathbf{Z}_k| \sim |(2d_kK)^{-1}(\mathbf{S}_x(f_k)+\mathbf{S}_y(f_k))| \prod_{l=1}^{p} U_l \tag{11}$$

where $U_l \sim (1/2)\chi^2_{2(d_kK-p+l)}$ and U_l's are independent.

Next we recall some useful results ([13, Result 1]):

Lemma 2. If $Z \sim \chi^2_n(\lambda)$, then $E\{Z\} = n + \lambda$. If $Y \sim \chi^2_n = \chi^2_n(0)$, then $E\{\ln Y\} = \psi(\frac{n}{2}) + \ln 2$ where $\psi(x) = d\,\ln\Gamma(x)/dx$ is the digamma function and $\psi(x) = \ln(x) - \frac{1}{2x} - \frac{1}{12x^2} + \cdots$. $\bullet$

Using Lemma 2, we have

$$E\{\ln|\mathbf{Z}_k|\} = E\left\{\ln\left|\frac{\mathbf{S}_x(f_k)+\mathbf{S}_y(f_k)}{2d_kK}\right| \prod_{l=1}^{p}\frac{1}{2}\chi^2_{2(d_kK-p+l)}\right\}$$

$$= -p\ln(d_kK) + \ln\left|\frac{\mathbf{S}_x(f_k)+\mathbf{S}_y(f_k)}{2}\right| + \sum_{l=1}^{p}\psi(d_kK-p+l), \tag{12}$$

$$E\{\ln|\mathbf{X}_k|\} = -p\ln K + \ln|\mathbf{S}_x(f_k)| + \sum_{l=1}^{p}\psi(K-p+l),$$

$$E\{\ln|\mathbf{Y}_k|\} = -p\ln K + \ln|\mathbf{S}_y(f_k)| + \sum_{l=1}^{p}\psi(K-p+l).$$

Using (7) and simplifying, we have

$$E\{2\ln(\mathcal{L}(\mathbf{X},\mathbf{Y}))\,|\,\mathcal{H}_1\} = 2K\sum_{k=1}^{M}\Big\{2\ln\left|\frac{\mathbf{S}_x(f_k)+\mathbf{S}_y(f_k)}{2}\right| - \ln|\mathbf{S}_x(f_k)| - \ln|\mathbf{S}_y(f_k)| - 2p\ln(d_k) + 2A_k\Big\}, \tag{13}$$

$$A_k := \sum_{l=1}^{p}\left\{\psi(d_kK-p+l) - \psi(K-p+l)\right\}. \tag{14}$$

Using Lemma 2 and after some tedious algebra

$$A_k = p\ln(d_k) + \frac{p}{d_kK} + \frac{p^2}{2K}\left[1-\frac{1}{d_k}\right] - \frac{p}{2K} + \mathcal{O}(K^{-2}). \tag{15}$$

It then follows that for "large" N, K, M, we have the non-centrality parameter

$$\begin{aligned}\lambda &= E\{2\ln(\mathcal{L}(\mathbf{X},\mathbf{Y}))\,|\,\mathcal{H}_1\} - Mp^2\\ &= 2K\sum_{k=1}^{M}\Big\{2\ln\left|\frac{\mathbf{S}_x(f_k)+\mathbf{S}_y(f_k)}{2}\right| - \ln(|\mathbf{S}_x(f_k)|) - \ln(|\mathbf{S}_y(f_k)|)\Big\}\\ &\quad + Mp^2 - 2pM - 2p(p-2)\left(\sum_{k=1}^{M}\frac{1}{d_k}\right).\end{aligned} \tag{16}$$

Remark 1. Under $\mathcal{H}_0$, the distribution $\chi^2_{Mp^2}$ is often not accurate, hence the extra terms and factor ρ in Theorem 1. Just as Theorem 1 modifies the distribution under $\mathcal{H}_0$, we will simply mimic (8) to modify the distribution $\chi^2_{Mp^2}(\lambda)$ under $\mathcal{H}_1$ exploiting Theorem 1:

$P\{2\rho\,\ln(\mathcal{L}) \le \tau\,|\,\mathcal{H}_0\}$ is given by (8),

$$\begin{aligned}P\{2\rho\,\ln(\mathcal{L}) \le \tau\,|\,\mathcal{H}_1\} &= P\{\chi^2_f(\rho\lambda) \le \tau\}\\ &+ \omega_2\big[P\{\chi^2_{f+4}(\rho\lambda)\le\tau\} - P\{\chi^2_f(\rho\lambda)\le\tau\}\big]\\ &+ \omega_3\big[P\{\chi^2_{f+6}(\rho\lambda)\le\tau\} - P\{\chi^2_f(\rho\lambda)\le\tau\}\big]\\ &+ \Big\{\omega_4\big[P\{\chi^2_{f+8}(\rho\lambda)\le\tau\} - P\{\chi^2_f(\rho\lambda)\le\tau\}\big]\\ &+ \frac{1}{2}\omega_2^2\big[P\{\chi^2_{f+8}(\rho\lambda)\le\tau\} - 2P\{\chi^2_{f+4}(\rho\lambda)\le\tau\}\\ &+ P\{\chi^2_f(\rho\lambda)\le\tau\}\big]\Big\} + \mathcal{O}(K^{-5})\end{aligned} \tag{17}$$

where $f = Mp^2$ and λ is given by (16). Under $\mathcal{H}_0$, $\lambda = 0$ and under $\mathcal{H}_1$, as signal gets weaker, $\lambda \to 0$; under both these cases (8) and (17) become the same. Also, as $N \to \infty$, we have $\rho \to 1$ and $\omega_r \to 0$ for $r = 2, 3, \cdots$, and we get $2\,\ln\mathcal{L} \sim \chi^2_{Mp^2}$ under $\mathcal{H}_0$ and $\sim \chi^2_{Mp^2}(\lambda)$ under $\mathcal{H}_1$. $\square$

6. SIMULATION EXAMPLES

6.1. Authentication

Recently researchers [15], [6] have proposed exploitation of physical layer approaches to enhance wireless security by using the unique wireless channel state information (CSI) of a legitimate user to authenticate subsequent transmissions from this user, thereby denying access to any spoofer whose CSI would significantly differ from that of the legitimate user by virtue of a different spatial location.Let $\{x(t)\}$ and $\{y(t)\}$ denote the received (sampled) downconverted scalar complex signals for the first frame (authenticated) and the second frame (yet to be authenticated), respectively. Then in the formulation of comparison of random signals [12, 14], one is interested in testing if $\{x(t)\}$ and $\{y(t)\}$ have the same PSDs. By limiting one's attention to direct comparison of the two time series, one avoids the additional burden of symbol timing synchronization and training sequence knowledge. Our formulation in this paper extends the approach of [12, 14] to multiple antenna receivers.

A random time- and frequency-selective Rayleigh fading $p \times 1$ vector channel $\mathbf{h}(n; l)$ (it is time-varying in simulations) is considered with 5 taps, equal power delay profile, mutually independent components, symbol interval $T_s = 1\,\mu$s with QPSK modulation and a Doppler spread f_d of 40 Hz. For different l's, $\mathbf{h}\,(n; l)$'s are mutually independent and satisfy Jakes' model (spectrum). The additive noise was zero-mean complex white Gaussian filtered through a linear filter with impulse response $\{0.6, 1.0, 0.6\}$. Unless otherwise noted, we also added artificial noise as discussed in Sec. 4. There are two frames of 256 symbols each (duration 256 μs) with a "gap" of 256 symbols. That is, first the "authenticated" user transmits a frame of 256 symbols; 256 μs later another frame is received. In simulations, when the second frame originates from the authentic user, in each run we generate a "long" doubly-selective channel spanning both frames and with the specified parameters. When the second frame is from the spoofer, in each run an independent doubly-selective channel is generated just for the second frame.

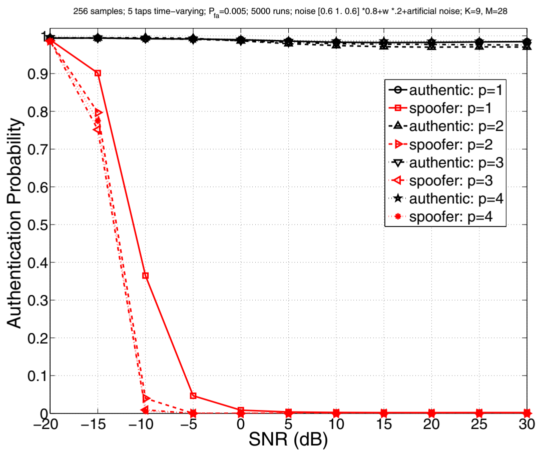

Fig. 1. *Time-varying channel of length =5 taps: Authentication probability refers to fraction of runs (out of 5000) in which the user was declared to be authentic. The curve labeled "authentic" refers to the case where the second message originated from the author of the first message. The curve labeled "spoofer" refers to the case where the second message originated from a spoofer. The results are based on 5000 runs, design $P_{fa} = 0.005$, colored noise, $N = 256$, $K = 9$, $M = 28$, channel length of 5 taps, Doppler spread of 40Hz for the authentic user while the spoofer is stationary.*

We picked $P_{fa} = 0.005$, $K = 9$ and $M = 28$ to design the test (to pick the threshold η). Fig. 1 shows our authentic user detection probability results where authentic user detection probability refers to fraction of runs (out of 5000) in which the authentic user was selected by the proposed test. Fig. 1 shows the results for a 5 tap authentic user channel with a Doppler spread of 40 Hz under colored Gaussian noise and varying SNR's for various values of number of receive antennas $p = 1, 2, 3, 4$. Two cases are depicted in Fig. 1: the curves labeled "authentic" is obtained when the second frame originates from the authentic user; the curves labeled "spoofer" are obtained when the second frame originates from a spoofer. It is seen from Fig. 1 that increasing the number of antennas from $p = 1$ to $p = 2$ yields a substantial improvement in SNR threshold at which spoofer can be correctly identified. With increasing noise (lower SNR's), it becomes much harder to distinguish between authentic user and spoofer.

6.2. Corroboration of Performance Analysis

Here we compare the theoretical performance based on the results of Sec. 5 with the simulations-based performance for the proposed detector. Fig. 2 shows the probability of detection (probability of detecting the spoofer when the second message originates from a spoofer) versus SNR results based on 5000 runs under the set-up for Fig. 1 except that the channels are time-invariant and after having been randomly generated, were then fixed for all runs – the results of Sec. 5 apply to processes with fixed PSDs. It is seen from Fig. 2 that the agreement between the theoretical and simulation-based results is good although not "perfect."

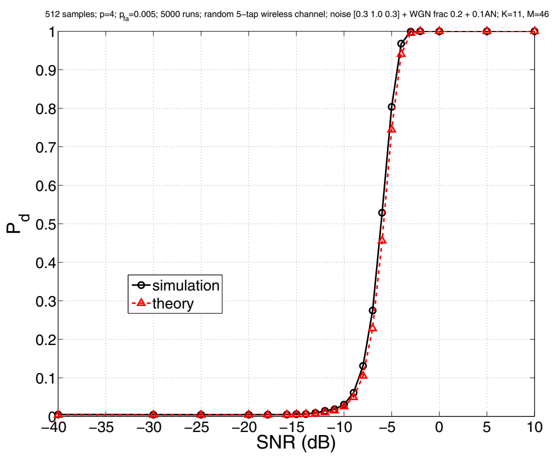

Fig. 2. *Corroboration of the theoretical performance analysis for the proposed approach based on 5000 runs: P_d vs SNR, P_{fa} = 0.005, $N = 512$, $K = 11$, $M = 46$.*

7. CONCLUSIONS

We analyzed the performance of the GLRT of [13] by deriving an approximate asymptotic distribution of the test statistic under the alternative hypothesis. We also provide robustification of this approach by adding artificial white noise to the received noisy signals. The results are illustrated via computer simulations which include application to user authentication in wireless networks with multiantenna receivers.

8. REFERENCES

[1] H.H. Andersen, M. Hojbjerre, D. Sorensen, and P.S. Eriksen, *Linear and Graphical Models for the Multivariate Complex Normal Distribution*, Lec. Notes Stat., vol. 101. New York: Springer-Verlag, 1995.

[2] D.R. Brillinger, *Time Series: Data Analysis and Theory*, Expanded edition. New York: McGraw Hill, 1981.

[3] T.S. Ferguson, *A Course in Large Sample Theory*, Chapman & Hall: London, 1996.

[4] K. Fokianos and A. Savvides, "On comparing several spectral densities," *Technometrics*, vol. 50, no. 3, pp. 317-331, Aug. 2008.

[5] T. Hayakawa, "The likelihood ratio criterion for a composite hypothesis under a local alternative," *Biometrika*, vol. 62, no. 2, pp. 451-460, Aug. 1975.

[6] Z. Li, W. Xu, R. Miller and W. Trappe, "Securing wireless systems via lower layer enforcements," in *Proc. 5th ACM Workshop Wireless Security (WiSe '06)*, pp. 33-42, Sept. 2006.

[7] R. Lund, H. Bassily and B. Vidakovic, "Testing equality of stationary autocovariances," *J. Time Series Anal.*, vol. 30, pp. 332-348, 2009.

[8] D.G. Nel and C.A. Van Der Merwe, "A solution to the multivariate Behrens-Fisher problem," *Communications in Statistics – Theory and Methods*, vol. 15, No. 12, pp. 3719-3735, 1986.

[9] D.B. Percival and A.T. Walden, *Spectral Analysis for Physical Applications*. Cambridge, UK: Cambridge Univ. Press, 1993.

[10] N. Ravishankar, J.R.M. Hosking and J. Mukhopadhyay, "Spectrum-based comparison of stationary multivariate time series," *Methodology and Computing in Applied Prob.*, vol. 12, pp. 749-762, 2010.

[11] A. Tani and R. Fantacci, "Low-complexity cyclostationary-based spectrum sensing for UWB and WiMAX coexistence with noise uncertainty," *IEEE Trans. Veh. Tech.*, vol. 59, pp. 2940-2950, July 2010.

[12] J.K. Tugnait, "Comparing random signals with application to wireless user authentication," in *Proc. 2011 45th Asilomar Conf. Signals, Systems & Computers*, Pacific Grove, CA, Nov. 6-9, 2011.

[13] J.K. Tugnait, "On comparing multivariate complex random signals," in *Proc. Intern. Conf. Signal Proc. Commun. (SPCOM 2012)*, pp. 1-5, Indian Institute of Science, Bangalore, India, July 22-25, 2012.

[14] J.K. Tugnait, "Wireless user authentication via comparison of power spectral densities," *IEEE J. Sel. Areas Commun.*, vol. 31, No. 9, pp. 1791-1802, Sept. 2013.

[15] L. Xiao, L.J. Greenstein, N.B. Mandayam and W. Trappe, "Using the physical layer for wireless authentication in time-variant channels," *IEEE Trans. Wireless Commun.*, vol. 7, pp. 2571-2579, July 2008.